

## 1 Supplementary information 1

### 2 Supplementary Methods

#### 3 *Location estimation from light-level loggers*

4 Estimated timings of sunrise and sunset (twilight transition times) were computed from light data using  
5 TransEdit2 (British Antarctic Survey/BAS, Cambridge, UK), and the `twilightCalc` function (GeoLight  
6 package; Lisovski & Hahn 2012) in R 3.3.3 (R Development Core Team 2017) for BAS, Migrate Technology  
7 and Biotrack loggers. Transition times were visually inspected for loggers retrieved during 2014-2017 by  
8 the same person. Lotek loggers did not retain raw light intensity data, but rather calculated and recorded  
9 latitudes and longitudes based on an on-board algorithm which has been shown to be biased  
10 (Frederiksen et al. 2016). Therefore we used these threshold method (Lisovski & Hahn 2012) derived  
11 positions to back calculate transition times using the `lotek_to_dataframe` function (`probGLS`  
12 package; Merkel et al. 2016). Daily experienced sea surface temperature (SST) was estimated from raw  
13 logged temperature data using the `sst_deduction` function (`probGLS` package) with a possible  
14 range of -2 to 20°C for Lotek loggers and -2 to 40°C for all other brands.

15 A most probable track for each individual and tracking year was calculated using an iterative method  
16 utilizing probability sampling detailed in Merkel et al. (2016) and implemented in the  
17 `prob_algorithm` function (`probGLS` package). Input data were logger recorded transition times,  
18 salt water immersion data as well as calculated daily recorded SST data. Daily optimal interpolated high  
19 resolution satellite derived SST, SST uncertainty estimates and sea ice concentration data for the  
20 algorithm with a 0.25° resolution were provided by NOAA (Boulder, Colorado, US; Reynolds et al. 2007).  
21 To improve precision we included land avoidance, an inability to enter the Baltic Sea (except for  
22 Common guillemots from the Isle of May) and an evasion of heavy pack ice (>90% sea ice concentration).  
23 Each movement path incorporated parameters based on the ecology of the species and the  
24 oceanographic conditions in the North Atlantic (table S1.1). Usually, it is not possible to estimate latitude  
25 during times of equinox as day length (the proxy for latitude) is very similar everywhere on earth.  
26 However, this methodology is able to estimate locations also during times of equinox by among other  
27 things utilizing the recorded temperature data and comparing them to satellite derived sea surface  
28 temperature (SST) fields. Due to small north-south gradients in SST in certain areas of the North Atlantic  
29 (e.g. the Gulf Stream along the Norwegian coast) we limited the boundary box parameter in

30 `prob_algorithm` for certain individuals and colonies after initial assessment of their movement track  
31 (table S1.1). Each computed track was afterwards visually inspected and erroneous locations particularly  
32 around polar night and midnight sun were removed (<1 % of all locations).

### 33 *Environmental parameters*

34 All chosen environmental parameters used to calculate the environmental space and their rationale are  
35 listed in table S1.3. Fronts in sea surface temperature (SST) and sea surface height anomaly fields were  
36 calculated using a canny edge detector (package `imager`, low & high threshold at 90% & 98%,  
37 respectively). Bathymetry was log-transformed and all distance measurements were capped at 500 km  
38 as well as square root-transformed. Predictability in SST was calculated as the sum of constancy and  
39 contingency following Colwell (1974) over a ten year time period (2007-2016) with 10 equal bins using  
40 the `hydrostats` package (figure S1.1). All variables have been standardized (variance = 1, mean = 0).

### 41 *Mantel correlation analysis*

42 Following Cohen et al. (2018) we calculated species-specific Mantel correlations to validate our  
43 migratory connectivity results with an independent method. All individual annual tracks were split into  
44 10 day bins starting 1 July. A resolution of 10 days was chosen to retain a sufficient number of locations  
45 for each bin for further analysis. Migratory connectivity for each species was quantified using Mantel  
46 correlation tests with 1000 permutations (Ambrosini et al. 2009). More specifically, the distance  
47 between individual breeding locations was compared to the distance between their current locations  
48 throughout the non-breeding season for each 10 day bin (as central location in each 10 day bin). For this  
49 analysis only data from the last three years of tracking was used (2014/15 - 2016/17) due to the uneven  
50 sampling across colonies in earlier years. To avoid pseudo-replication only one year of tracking for each  
51 repeat track individual was used (randomly chosen). Further, ecoregion- and season-specific Mantel  
52 correlation tests were computed - for ecoregions with individuals from more than one population  
53 present during the focal time period - to assess the area and season specific connectivity for each  
54 species. Results are illustrated in figure S1.3.

55

## 56 **Supplementary references**

57 Amante C, Eakins BW (2009) ETOPO1 1 Arc-Minute Global Relief Model: Procedures, Data  
58 Sources and Analysis. NOAA Technical Memorandum NESDIS NGDC-24. National  
59 Geophysical Data Center, NOAA. . Accessed 2015-07-17.

- 60 Ambrosini R, Møller AP, Saino N (2009) A quantitative measure of migratory connectivity.  
61 *Journal of Theoretical Biology* 257:203-211
- 62 Berrisford P, Dee D, Poli P, Brugge R, Fielding K, Fuentes M, Kallberg P, Kobayashi S, Uppala S,  
63 Simmons A (2011) The ERA-Interim archive Version 2.0, ERA Report Series 1, ECMWF,  
64 Shinfield Park. Reading, UK 13177
- 65 Biotrack (2013) M-Series Geolocator User Manual V11.
- 66 Cavalieri DJ, Parkinson CL, Gloersen P, Comiso JC, Zwally HJ (1999) Deriving long-term time  
67 series of sea ice cover from satellite passive-microwave multisensor data sets. *Journal of*  
68 *Geophysical Research: Oceans* 104:15803-15814
- 69 Cohen EB, Hostetler JA, Hallworth MT, Rushing CS, Sillett TS, Marra PP (2018) Quantifying the  
70 strength of migratory connectivity. *Methods Ecol Evol* 9:513-524
- 71 Colwell RK (1974) Predictability, Constancy, and Contingency of Periodic Phenomena. *Ecology*  
72 55:1148-1153
- 73 Elliott KH, Gaston AJ (2005) Flight speeds of two seabirds: a test of Norberg's hypothesis. *Ibis*  
74 147:783-789
- 75 Fort J, Porter WP, Grémillet D (2009) Thermodynamic modelling predicts energetic bottleneck  
76 for seabirds wintering in the northwest Atlantic. *The Journal of Experimental Biology*  
77 212:2483-2490
- 78 Frederiksen M, Descamps S, Erikstad KE, Gaston AJ, Gilchrist HG, Grémillet D, Johansen KL,  
79 Kolbeinsson Y, Linnebjerg JF, Mallory ML, McFarlane Tranquilla L, Merkel FR,  
80 Montevecchi WA, Mosbech A, Reiertsen TK, Robertson GJ, Steen H, Strøm H,  
81 Thórarinnsson TL (2016) Migration and wintering of a declining seabird, the thick-billed  
82 murre *Uria lomvia*, on an ocean basin scale: Conservation implications. *Biol Conserv*  
83 200:26-35
- 84 Jakobsson M, Mayer L, Coakley B, Dowdeswell JA, Forbes S, Fridman B, Hodnesdal H, Noormets  
85 R, Pedersen R, Rebesco M, Schenke HW, Zarayskaya Y, Accettella D, Armstrong A,  
86 Anderson RM, Bienhoff P, Camerlenghi A, Church I, Edwards M, Gardner JV, Hall JK, Hell  
87 B, Hestvik O, Kristoffersen Y, Marcussen C, Mohammad R, Mosher D, Nghiem SV,  
88 Pedrosa MT, Travaglini PG, Weatherall P (2012) The International Bathymetric Chart of  
89 the Arctic Ocean (IBCAO) Version 3.0. *Geophysical Research Letters* 39
- 90 Lisovski S, Hahn S (2012) GeoLight – processing and analysing light-based geolocator data in R.  
91 *Methods Ecol Evol* 3:1055-1059
- 92 Lisovski S, Hewson CM, Klaassen RHG, Korner-Nievergelt F, Kristensen MW, Hahn S (2012)  
93 Geolocation by light: accuracy and precision affected by environmental factors. *Methods*  
94 *Ecol Evol* 3:603-612
- 95 Lumpkin R, Johnson GC (2013) Global ocean surface velocities from drifters: Mean, variance, El  
96 Niño–Southern Oscillation response, and seasonal cycle. *Journal of Geophysical*  
97 *Research: Oceans* 118:2992-3006
- 98 Merkel B, Phillips RA, Descamps S, Yoccoz NG, Moe B, Strøm H (2016) A probabilistic algorithm  
99 to process geolocation data. *Movement Ecology* 4:26
- 100 R Development Core Team (2017) R: A language and environment for statistical computing. R  
101 Foundation for Statistical Computing, Vienna, Austria
- 102 Reynolds RW, Smith TM, Liu C, Chelton DB, Casey KS, Schlax MG (2007) Daily High-Resolution-  
103 Blended Analyses for Sea Surface Temperature. *Journal of Climate* 20:5473-5496

104 Scales KL, Miller PI, Hawkes LA, Ingram SN, Sims DW, Votier SC (2014) REVIEW: On the Front  
105 Line: frontal zones as priority at-sea conservation areas for mobile marine vertebrates.  
106 *Journal of Applied Ecology* 51:1575-1583

107

108 **Supplementary Tables and Figures**

109

110 **Table S1.1.** probGLS algorithm input parameters used to compute locations. standard deviation = sd

algorithm parameter	description	value used
particle.number	number of particles computed for each point cloud	2000
iteration.number	number of track iterations	100
loess.quartile	remove outliers in transition times based on local polynomial regression fitting processes (Lisovski & Hahn 2012)	used with k = 10
sunrise.sd & sunset.sd	shape, scale and delay values describing the assumed uncertainty structure for each twilight event following a log normal distribution	2.49/ 0.94/ 0 <sup>1</sup>
range.solar	range of solar angles used	-7° to -1° (except for C250 logger from SK: -4° to -2°)
boundary.box	the range of longitudes and latitudes likely to be used by tracked individuals	90°W to 120°E & 40°N to 81°N; except for 91% COGU tracks from IM with 40°N to 62°N; all COGU from BI and 94% COGU SK tracks with 60°N to 77°N; 6% SK tracks with 50°N to 77°N
day.around.spring.equinox & days.around.fall.equinox	number of days before and after an equinox event in which a random latitude will be assigned	spring: 21 days before & 14 days after autumn: 14 days before & 21 days after
speed.dry	fastest most likely speed, speed sd and maximum speed allowed when the logger is not submerged in sea water	17/ 4/ 30 m/s <sup>2</sup>
speed.wet	fastest most likely speed, speed sd and maximum speed allowed when the logger is submerged in sea water	1/ 1.3/ 5 m/s <sup>3</sup>
sst.sd	logger-derived sea surface temperature (SST) sd	0.5°C <sup>4</sup>
max.sst.diff	maximum tolerance in SST variation	3°C
east.west.comp	compute longitudinal movement compensation for each set of twilight events (Biotrack 2013)	used

111

112 <sup>1</sup> These parameters are chosen as they resemble the twilight error structure of open habitat species in Lisovski et al. (2012).

113 <sup>2</sup> inferred from GPS tracks (unpublished data) and (Elliott & Gaston 2005)

114 <sup>3</sup> North Atlantic current speed up to fast current speeds (i.e. East Greenland current) (Lumpkin & Johnson 2013) as the tagged animal is assumed to not actively move when the logger is immersed in seawater

115 <sup>4</sup> logger temperature accuracy

116

117 **Table S1.2.** Proportion of locations missing in each season mainly due to lack of twilight events caused by  
 118 midnight sun (seasons: autumn and spring) or polar night (early and late winter) for each breeding  
 119 population as well as mean and standard deviation (sd) across populations. Breeding populations: SNZ =  
 120 Southern Novaya Zemlya, NNZ = Northern Novaya Zemlya, ESP = Eastern Spitsbergen, WSP = Western  
 121 Spitsbergen, BI = Bjørnøya, SBS = Southern Barents Sea, HJ = Hjelmsøya, SK = Sklinna, JM = Jan Mayen, IC  
 122 = Northeast Iceland, FA = Faroe Islands, IM = Isle of May

species	season	breeding populations												mean	sd
		IM	FA	SK	IC	JM	WSP	HJ	BI	SBS	ESP	SNZ	NNZ		
BRGU	autumn	-	-	-	15 %	13 %	39 %	-	29 %	15 %	58 %	11 %	47 %	29 %	17 %
	early winter	-	-	-	6 %	1 %	1 %	-	5 %	36 %	100 %	20 %	97 %	33 %	39 %
	late winter	-	-	-	0 %	2 %	1 %	-	3 %	4 %	29 %	1 %	8 %	6 %	9 %
	spring	-	-	-	30 %	45 %	73 %	-	63 %	45 %	91 %	51 %	81 %	60 %	19 %
COGU	autumn	1 %	2 %	10 %	0 %	8 %	-	12 %	14 %	4 %	-	-	-	6 %	5 %
	early winter	1 %	1 %	9 %	0 %	5 %	-	51 %	34 %	39 %	-	-	-	18 %	19 %
	late winter	1 %	0 %	1 %	1 %	3 %	-	2 %	5 %	2 %	-	-	-	2 %	2 %
	spring	4 %	12 %	14 %	31 %	46 %	-	44 %	48 %	27 %	-	-	-	28 %	16 %

123

124

125 **Table S1.3.** Parameter chosen to describe the environmental space.

parameter	temporal resolution	spatial resolution	rational	data source
bathymetry	static	0.25°	predictable productivity on continental shelves	ETOPO1 & IBCAO <sup>1</sup>
surface air temperature	daily	0.75°	influences energy requirements <sup>2</sup>	ECMWF <sup>3</sup>
sea surface temperature (SST)	daily	0.25°	water mass indicator & physiological constraint <sup>2</sup>	NOAA OI SST V2 <sup>4</sup>
SST predictability (figure S1.2)	static	0.25°	identifier of spatially variable SST features across seasons and years (e.g. persistent frontal systems <sup>5</sup> )	NOAA OI SST V2 <sup>4</sup>
minimum distance to 15%, 50% & 90% sea ice concentrations	daily	0.25°	descriptor of marginal sea ice zone	NSIDC <sup>6</sup>
sea surface height (SSH)	daily	0.25°	descriptor of the locations of large-scale features such as gyres and fronts	AVISO <sup>7</sup>
distance to SSH anomaly gradients	daily	0.25°	distance to meso-scale eddies as spatially dynamic sources of upwelling	AVISO <sup>7</sup>
distance to SST gradient	daily	0.25°	distance to meso- and large-scale temperature fronts <sup>5</sup>	NOAA OI SST V2 <sup>4</sup>

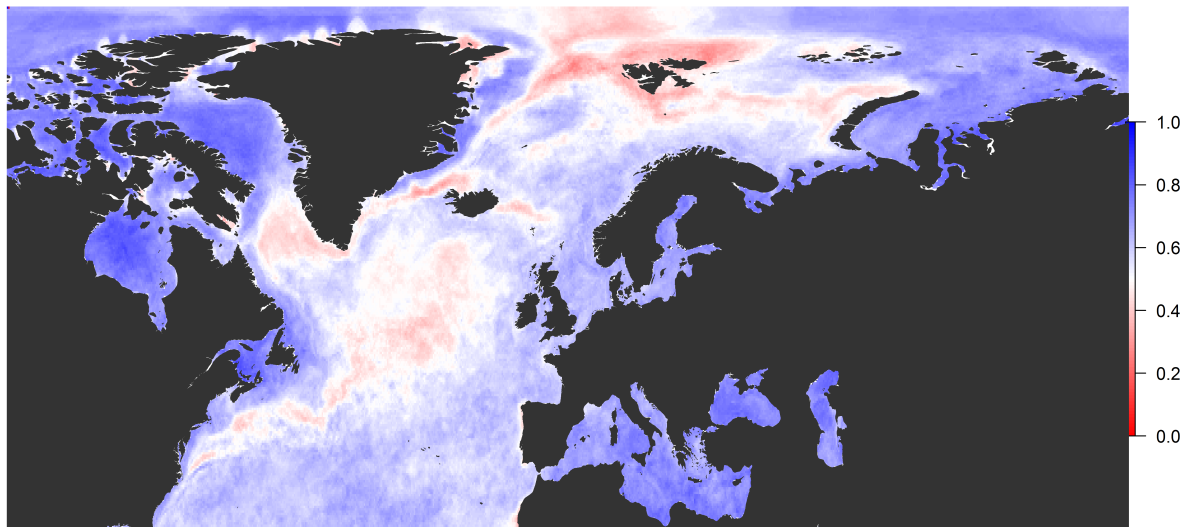
126 <sup>1</sup> (Amante & Eakins 2009, Jakobsson et al. 2012), <sup>2</sup> (Fort et al. 2009), <sup>3</sup> (Berrisford et al. 2011), <sup>4</sup> (Reynolds et al. 2007), <sup>5</sup> (Scales et  
 127 al. 2014), <sup>6</sup> (Cavalieri et al. 1999), <sup>7</sup> Aviso, with support from Cnes (<http://www.aviso.altimetry.fr/>)

128

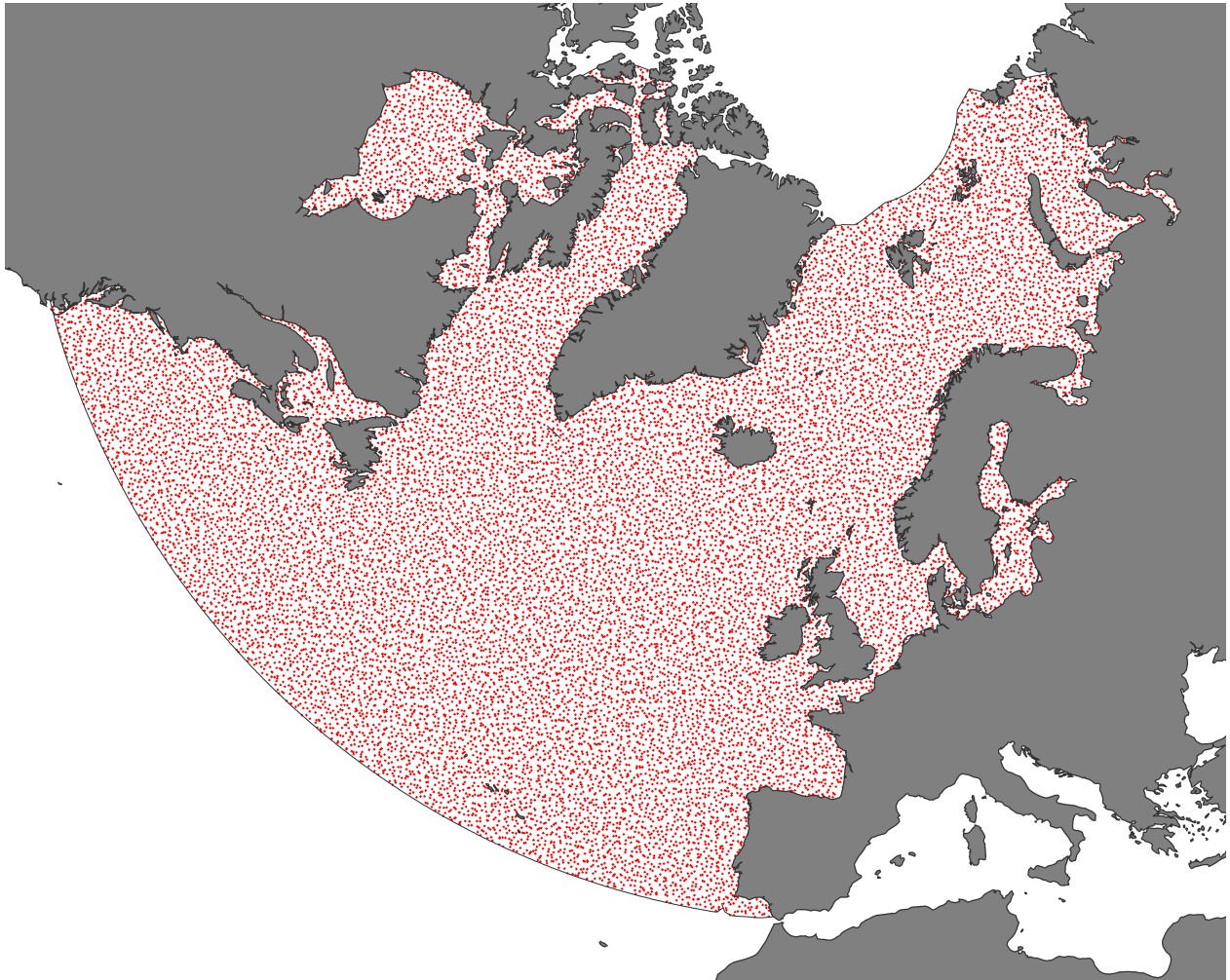
129  
 130 **Table S1.4.** Large-scale movement network metrics. P-values derived by two tailed t-tests. Displayed  
 131 values denote mean ± standard deviation (minimum & maximum in brackets), if not labelled otherwise.  
 132 df = degree of freedom  
 133

network metric	COGU	BRGU	p-value	df
# of nodes	24	25	-	-
# of populations present at a node	2.7 (1-7)	3.5 (1-6)	0.13	46
node size	17±14% (2-56%)	16±20% (0.4-75%)	0.89	42
node size by population	<b>49±40% (1-100%)</b>	<b>37±38% (1-100%)</b>	<b>0.05</b>	<b>134</b>
total degrees (connections per node)	<b>6.9 (2-21)</b>	<b>10.8 (2-26)</b>	<b>0.03</b>	<b>60</b>
edge size	7±8% (0.2-38%)	5±8% (0.1-55%)	0.14	157
edge size by population	<b>36±38% (1-100%)</b>	<b>22±32% (1-100%)</b>	<b>0.001</b>	<b>202</b>
# of unique ecoregions used by population	3.5 (2-6)	4.8 (2-8)	0.24	12
# of unique ecoregions used by individuals	<b>1.5±0.7 (1-4)</b>	<b>2.3±0.9 (1-4)</b>	<b>&lt;0.001</b>	<b>156</b>

134  
 135  
 136



137  
 138  
 139 **Figure S1.1.** Distribution of SST predictability in the North Atlantic with a scale from 0 (no predictability)  
 140 to 1 (very predictable).

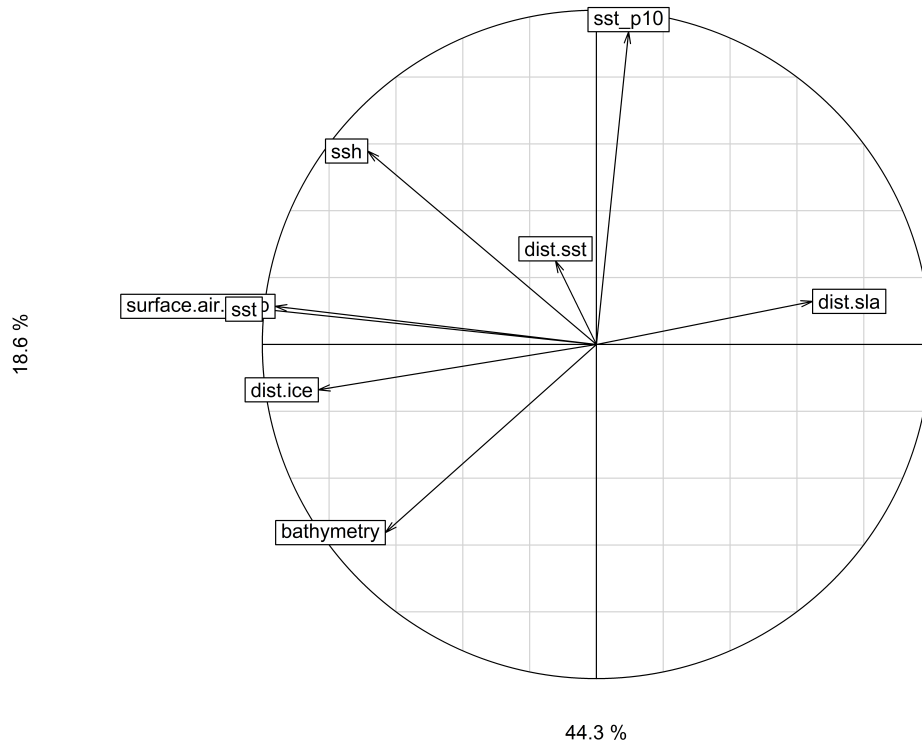


141

142 **Figure S1.2.** Map (in polar stereographic projection) displaying the study region including the 20000

143 random locations (in red) used to estimate the available environmental space.





144

44.3 %

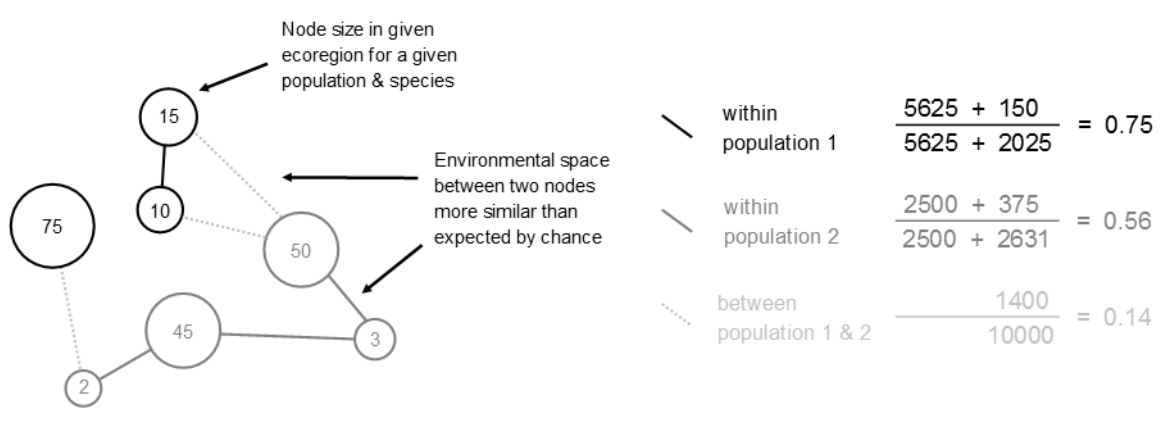
145 **Figure S1.3.** PCA correlation circle for the environmental space representing the North-Atlantic over the  
146 entire study period. dist.sla = distance to mesoscale eddies, dist.ice = distance to the marginal sea ice  
147 zone, surface.air.temp = surface air temperature, sst = sea surface temperature, ssh = sea surface height,  
148 dist.sst = distance to SST fronts, sst\_p10 = SST predictability

149

150

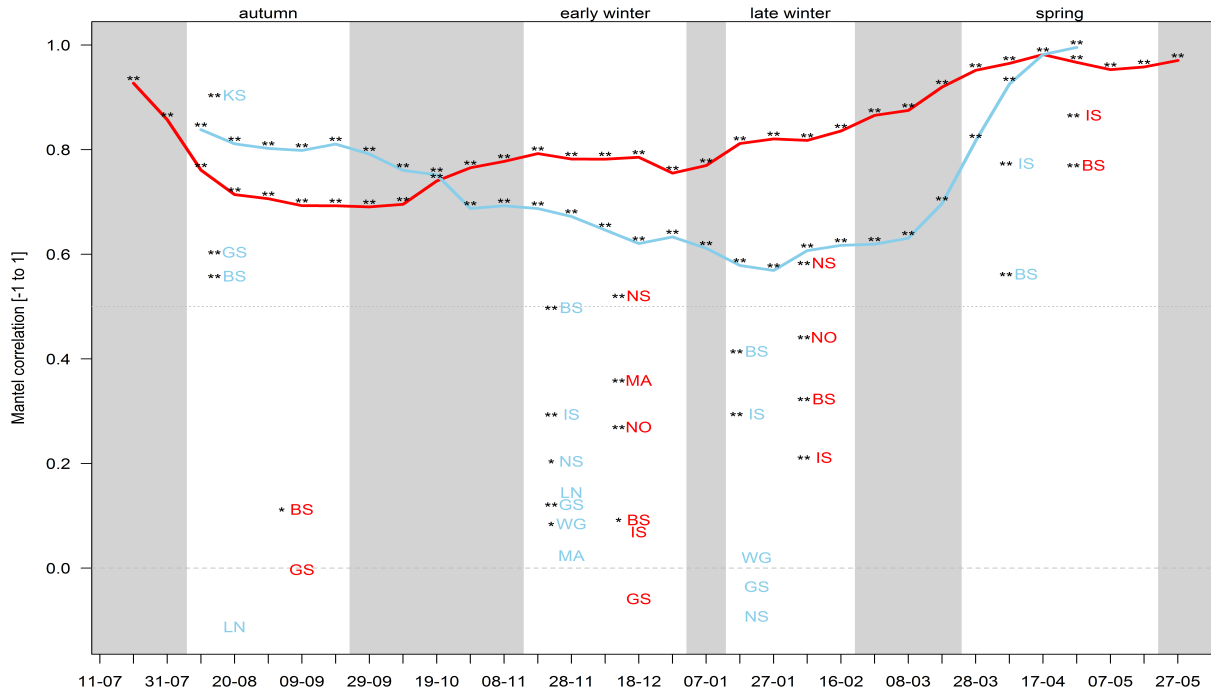
151

152



153

154 **Figure S1.4.** A schematic detailing the environmental similarity index (S) calculations in equation 1  
 155 (within example populations, solid lines) and equation 2 (between two example populations, dashed  
 156 lines) using two example populations (in black and grey). The symbols denote ecoregion-, species- and  
 157 breeding population-specific environmental space use. Its size corresponds to the proportional use as  
 158 visualised in figure 1B. Lines connect environmental spaces which are similar based on the  
 159 environmental niche similarity test (one way is considered sufficient, i.e. *niche* 1  $\cong$  *niche* 2 | *niche* 2  $\cong$   
 160 *niche* 1).  
 161



162  
163 **Figure S1.5.** Species-specific mantel correlation through time (10 day bins) for all data from 2014-2017.

164 BRGU in blue and COGU in red. Labels in each season (white boxes) denote season-specific mantel  
165 correlation values for each particular ecoregion with birds from more than one breeding population  
166 present. Significance levels based on 1 000 permutations: \*\* = <0.001, \* = <0.05; Ecoregion  
167 abbreviations: BS = Barents Sea, KS = Kara Sea, GS = Greenland Sea, IS = Iceland Shelf & Sea, WG = West  
168 Greenland, NO = North Sea, MA = Central North Atlantic, NS = Norwegian Sea, LN = Labrador shelf &  
169 Newfoundland

170

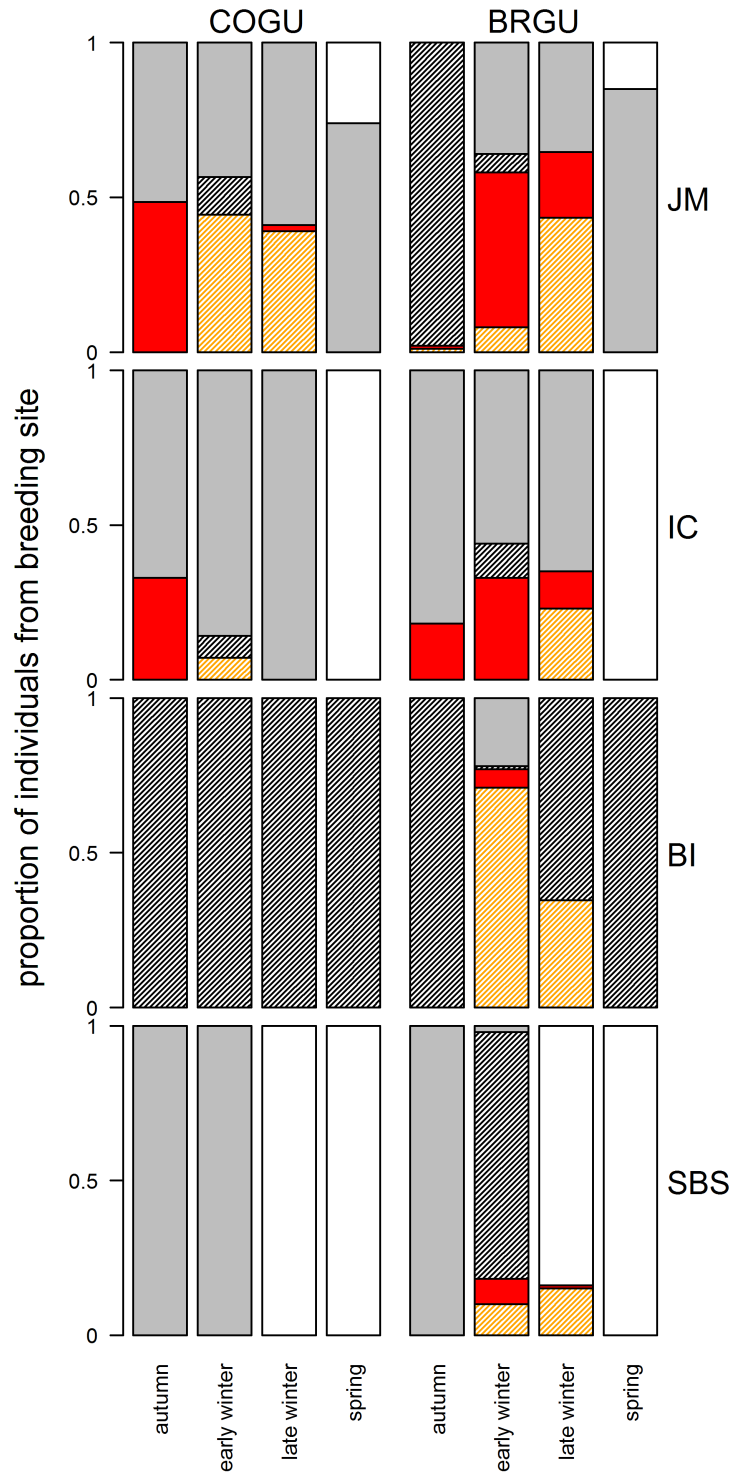


**Figure S1.6.** Seasonal proportional comparative space and environmental niche use between both species breeding sympatric at four breeding locations (JM = Jan Mayen, IC = North-East Iceland, BI = Bjørnøya & SBS = Southern Barents Sea). The proportion of the population occupying the same ecoregion with the other sympatric species breeding at the same location is indicated in white-grey-black colours while red-orange colours indicate different ecoregions used. Dark colours (grey & black) correspond to species-specific within ecoregion space use while white illustrates mixing between the species within ecoregions. Solid colours (white, grey & red) indicate similar environmental niches occupied while shaded colours denote distinct environments used (black & orange).